THE JOURNAL OF COMPARATIVE NEUROLOGY 421:199–214 (2000)

Tyrosine Phosphatase SHP-1 Immunoreactivity Increases in a Subset of Astrocytes Following Deafferentation of the Chicken Auditory Brainstem

DIANA I. LURIE,[1]* FLAVIO SOLCA,[2] EDMOND H. FISCHER,[2] AND EDWIN W RUBEL[1]

[1]Virginia Merrill Bloedel Hearing Research Center, Department of Otolaryngology-Head and Neck Surgery, University of Washington, Seattle, Washington 98195

[2]Department of Biochemistry, University of Washington, Seattle, Washington 98195

ABSTRACT

Proliferation of astrocytes is a dramatic response of the central nervous system (CNS) to injury and disease. Such proliferation results in the formation of the neural/glial scar and the reconstitution of the glial limitans. However, not all astrocytes enter the proliferative cycle following injury, and for those that do, the period of cell division is limited. Little attention has focused on the events that regulate the duration and extent of astrocyte proliferation following damage, but clearly control mechanisms are in place as CNS injury does not result in the continuous astrocyte proliferation seen in glial tumorigenesis. Protein tyrosine phosphorylation has been implicated in both astrocyte proliferation and differentiation and plays an important role in the regulation of the cell cycle in a number of different systems. We have found a small subset of astrocytes in the chick auditory brainstem that are immunopositive for the protein tyrosine phosphatase SHP-1. SHP-1 appears to negatively regulate cellular division in the hematopoietic system and is involved in the mitogenic response to various growth factors. Following cochlea removal, there is a marked increase within the auditory brainstem nucleus, nucleus magnocellularis (NM), in both in the number of SHP-1-positive astrocytes and the length of their immunopositive fibers. Significantly, those animals showing the greatest increases in SHP-1 immunoreactivity do not exhibit large amounts of astrocyte proliferation. We hypothesize that the expression of SHP-1 plays a role in negatively regulating the mitotic behavior of astrocytes following deafferentation. J. Comp. Neurol. 421:199–214, 2000. © 2000 Wiley-Liss, Inc.

Indexing terms: glia; injury; phosphorylation; proliferation; avian

Astrocyte proliferation and hypertrophy is a major hallmark of central nervous system (CNS) injury (Reier et al., 1983; Graeber and Kreutzberg, 1986, 1988; Reier and Houle, 1988; Tetzlaff et al., 1988; Condorelli et al., 1989; Steward et al., 1990). Proliferating astrocytes are believed to occupy the spaces left by degenerating neural cells, reconstitute the glial limitans, and form a neural/glial scar (Reier and Houle, 1988). Although the end result is well characterized, neither the signals that send astrocytes into the cell cycle following injury nor the basis on which certain astrocytes are induced to proliferate are well understood. Few studies have focused on those events that determine (1) which astrocytes will enter the cell cycle and (2) the duration and extent of astrocyte proliferation following CNS injury. Gaining insight into the cellular cascades that control astrocyte entry into, as well as exit from, the cell cycle is an important focus area for the development of new strategies leading to functional recovery following injury.

Accumulating evidence points to the role of protein phosphorylation and dephosphorylation in cell cycle reg-

Dr. Lurie's current address is: Department of Pharmaceutical Sciences, University of Montana, Missoula, MT.

Dr. Solca's current address is: Boehringer Ingelheim, Vienna, Austria.

*Correspondence to: Diana I. Lurie, Department of Pharmaceutical Sciences, University of Montana, 32 Campus Dr. #1552, Missoula, MT 59812-1552. E-mail: Lurie@selway.umt.edu

Received 13 October 1999; Revised 20 January 2000; Accepted 21 January 2000

© 2000 WILEY-LISS, INC.

ulation. Dephosphorylation events, in particular, have been implicated in the inhibition of cell division, although this negative regulation depends on the individual phosphatase and the cellular environment in which it is expressed (Lau and Baylink, 1993; Neel, 1993). Interestingly, tyrosine phosphorylation is believed to play a role in the regulation of both astrocyte proliferation and differentiation (Ingraham and Maness, 1990; Harrison and Mobley, 1991). Several growth factors that activate protein tyrosine kinase receptors (i.e., fibroblast growth factor [FGF], epidermal growth factor [EGF], platelet-derived growth factor [PDGF], interleukin-1 [IL-1], and insulin-like growth factor [IGF]) have recently been shown to be mitogenic for astrocytes in vitro (Huff and Scheier, 1990; for review, see Malhotra et al., 1990; Langan et al., 1994). However, the role of tyrosine phosphorylation in regulating astrocyte proliferation following injury has not been closely examined. In the present study, tyrosine phosphatase antibodies were used to determine whether the expression of the tyrosine phosphatase, SHP-1, is altered in response to loss of neural activity in the chicken auditory brainstem.

Neurons in the chicken cochlear nucleus, nucleus magnocellularis (NM), receive their only excitatory input from the eighth nerve. Removal of the cochlea results in both astrocyte proliferation and hypertrophy on the deafferented side (Canady and Rubel, 1992; Rubel and MacDonald, 1992; Lurie and Rubel, 1994). Two antibodies directed against SHP-1 (also known as PTP1C, SHPTP-1, SHP, and HCP) were found to label a subset of astrocytes in the chicken brainstem. SHP-1 is a cytoplasmic phosphatase containing two SH2 domains located within the N-terminus of the protein and is highly expressed in hematopoietic cells (Shen et al., 1991).

In the present study, chickens received a unilateral cochlea removal and brainstem sections were stained with the SHP-1 antibodies. A subset of astrocytes within NM display an increase in SHP-1 immunostaining following cochlear removal. By 36 hours postablation, significantly more SHP-1-positive (SHP-1+) astrocytes are found in NM compared with the contralateral (undamaged) brainstem. Moreover, those animals that show large increases in SHP-1 immunoreactivity exhibit less proliferation than those animals that show lower levels of SHP-1 immunoreactivity. This suggests that SHP-1 plays a role in negatively regulating astrocyte proliferation following injury. Portions of this study have been presented in abstract form (Lurie et al., 1993; Kosena and Lurie, 1997).

MATERIALS AND METHODS

Animals

Posthatch chickens (7–21 days old) were used for all experiments. White leghorn eggs were obtained from a local supplier (H&N Farms, Redmond, WA) and incubated in the University of Washington vivarium in AAALAC-approved facilities. One-day-old hatchlings were also obtained from the Privett Hatchery (Portales, NM) and maintained in the University of Montana vivarium in AAALAC-approved facilities. Animals were maintained in warm brooders with a 12-hour light/dark cycle, constant temperature and humidity, and they were given free access to food and water at all times.

Surgical procedures

Chickens were deeply anesthetized with a combination of ketamine (80 mg/kg body weight intramuscularly [IM]) and sodium pentobarbital (15 mg/kg body weight intraperitoneally [IP]) or xylazine (1 mg per animal IP). Surgical removal of the basilar papilla (cochlea) has been previously described (Born and Rubel, 1985; Durham and Rubel, 1985). In summary, the feathers around the ear canal were removed, the tympanic membrane punctured and reflected, and the columella removed from the middle ear. The cochlea was then extracted though the oval window with a pair of fine forceps and examined under a dissecting microscope to ensure complete removal. The cavity of the oval window was filled with gelfoam and the incision sealed with cyanoacrylate glue. All procedures were carried out under aseptic conditions. Following the unilateral cochlea removal, animals were allowed to survive for 6, 12, 24, 36, 72 hours, 5 days, 7 days, 10 days, and 13 days ($n = 3–6$ per time point). Age-matched controls were anesthetized but received no cochlear removal. One group of animals ($n = 2$) received a unilateral cochlea removal and 48 hours later received a single injection of the thymidine analog, bromodeoxyuridine (BrdU; 5 mg/100 g body weight). This group of animals was sacrificed 6 hours after the BrdU injection. Another group of animals received a unilateral cochlea removal and were given BrdU injections twice daily on days 2–3 ($n = 3$), 5–6 ($n = 3$), and 8–9 ($n = 2$) after deafferentation. These animals were sacrificed 6 hours following the final injection of BrdU.

Immunohistochemistry for SHP-1

At 6, 12, 24, 36, 72 hours, 5 days, 7 days, 10 days, and 13 days after cochlea removal, the chickens were deeply reanesthetized and transcardially perfused with chick Ringer's (154 mM NaCl, 6 mM KCl, 8.4 mM $MgCl_2$, 5 mM HEPES, 8 mM glucose, 1 mM EGTA) for 3 minutes. The brains were removed and postfixed in a modified Carnoy's fix (6 parts 100% ethanol, 2 parts chloroform, 1 part glacial acetic acid, and 1 part 10× chick Ringer's) at 4°C for 6 hours. Following fixation, the brains were rinsed in 70% ethanol, left in 70% ethanol overnight, and embedded in paraffin the next day. Ten-micron sections were cut, and a 1 in 4 series mounted onto bleach-washed, chrome Alum-subbed slides, and deparaffinized. Sections were then processed for SHP-1 immunohistochemistry with either the 205 or 196 antibody. We have used two different anti-SHP-1 antibodies (205 and 196 antisera) that label a subset of astrocytes in the normal and deafferented chick brainstem. The 205 and 196 antisera were provided by Dr. Shen (Montreal, Canada). The 205 antibody is generated against the whole SHP-1 protein and the 196 antiserum is generated against a peptide derived from Leu211-ASN221 of SHP-1 (Dr. Shen, personal communication). Both antisera recognize the SHP-1 enzyme in the chicken brain.

For 205 and 196 immunohistochemistry, all sections were rinsed in Tris buffer (pH 7.4) and Tris buffer with bovine serum albumin (BSA; pH 7.4, Sigma, St. Louis, MO) and then blocked with 4% normal goat serum for 20 minutes. This and all other immunocytochemical reagents (except for the avidin-biotin complex [ABC] reagent) were prepared in 1% BSA/0.1% sodium azide in Tris buffer (pH 7.4). The sections were then incubated overnight in either the 205 or the 196 antibody (1:4,000-205; 1:3,000-196) at

4°C. Alternate sections were incubated overnight with anti-glial fibrillary acidic protein (1:600-GFAP; Dako, Carpinteria, CA). The next day, the sections were rinsed in the Tris buffers, incubated in 1:400 biotinylated goat anti-rabbit serum (Vector Labs, Burlingame, CA) for 1 hour, rinsed in Tris, and then incubated with the ABC (Vectastain ABC elite kit, Vector Labs). The chromagen used was diaminobenzedine (DAB 0.25; Sigma) and 0.001 M imidazole and 0.1% hydrogen peroxide in Tris buffer.

Double-label immunohistochemistry for SHP-1 and BrdU

Paraffin sections from animals that had received the BrdU injections were first processed for BrdU immunohistochemistry. This was similar to the 205 and 196 immunohistochemistry described above with the following exceptions: (1) sections were first immersed in ddH_2O for 10 minutes, and then immersed in 1N HCl for 20 minutes; (2) sections were blocked with 4% normal horse serum and incubated overnight in anti-BrdU (1:300, Becton Dickinson, San José, CA) at room temperature; (3) sections were incubated in biotinylated horse anti-mouse serum; and (4) the DAB chromagen was intensified with 0.08% nickel chloride to create a black rather than brown reaction product. Following processing for BrdU immunohistochemistry, sections were then double labeled with either the 205 or the 196 antiserum as described above. The sections were then dehydrated and coverslipped.

Tissue analysis

Brainstem sections were viewed with a Zeiss Universal microscope at a final magnification of 260×. The density of the 205 and 196 reaction product within NM was determined using NIH Image Analysis Program 1.45.

With a random start, every eighth section through the NM was analyzed. Slides were viewed with a microscope attached to a Dage-MTI (Michigan City, IN) Model 68 video camera connected to a Macintosh IIcx computer. A Datatranslation QuickCapture board (Datatranslation, Marlboro, MA) was used to capture the image from the microscope. NIH Image 1.45 (image analysis software) allowed the analysis of the digitized images. A brainstem image, including the entire NM, was captured onto the computer screen. The boundary of NM was outlined and a threshold was set such that the reaction product within NM reached this threshold whereas the surrounding unstained tissue did not. The number of pixels that reached threshold within the outlined region was then calculated by the computer. The same procedure was repeated for the contralateral NM without changing the threshold setting. The area of staining within the deafferented (ipsilateral) NM was then divided by the area of staining within the control (contralateral NM). In this way, increases in the area of staining between the deafferented and control NM in the same tissue section could be calculated and expressed as a ratio. New thresholds were set for each tissue section. These ratios were then averaged over all sections measured within each brain to determine a single value for each brain. Significant differences in the area of staining of 205 and 196 reaction product were determined by a one-way analysis of variance (ANOVA).

Biochemistry

Tissue extraction. Fifteen to twenty chickens aged 7–21 days were decapitated and the brains quickly removed and placed on ice. The tissue was then washed in phosphate-buffered saline (PBS; pH 7.4) and homogenized in a Waring (New Hartford, CT) blender with 4 volumes of extraction buffer (25 mM imidazole, pH 7.2, 10% glycerol, 0.1% β-mercaptoethanol, 2 mM EDTA, 2 mM EGTA, 1% Triton X, 1 mM benzamidine, 0.002% phenylmethylsulfonyl fluoride (PMSF) [w/v], 2 μg/ml leupeptin, 0.5 μg/ml pepstatin A, and 20 KIU/ml aprotinin). The homogenate was centrifuged at 100,000 g for 20 minutes at 4°C and the supernatant collected.

Anion exchange chromatography. An aliquot of the supernatant (10 mg) was applied to a 5-ml Q Sepharose Fast Flow column (Pharmacia, Piscataway, NJ), equilibrated in buffer A (25 mM Tris-HCl, pH 7.5, 1 mM EDTA, 1 mM β-mercaptoethanol), and then washed with 20 ml of buffer A. The column was developed with a linear gradient of buffer B (buffer A supplemented with 1 M NaCl; 0–100% NaCl in 38 ml) with a flow rate of 0.5 ml per minute. Fractions of 0.75 ml were collected and the protein tyrosine phosphatase (PTP) activity profile was determined using (^{32}PY) myelin basic protein (MBP) as substrate.

Gel filtration. The Ab205-positive fractions were identified by Western blot analysis, pooled, and a 1-ml aliquot was applied to an analytical Superose 12 sizing column pre-equilibrated in buffer A with 50 mM NaCl. The flow rate was 0.5 ml per minute in the same buffer.

Western blots. The proteins in each fraction from both the Q Fast Flow and Superose 12 columns (50-μl samples) were separated on 10% polyacrylamide gels, transferred to nitrocellulose (Schleicher & Schuell, Keene, NH), blocked with 5% non-fat dry milk in TBST (20 mM Tris-HCl, pH 7.5, 150 mM NaCl, 0.05% Tween-20), and probed with the 205 antiserum diluted 1:1,000 in TBST-B (TBST with 0.1% BSA). After three washes in TBST, immunoreactive proteins were visualized with a secondary goat anti-rabbit IgG coupled to alkaline phosphatase (1:4,000; Bio-Rad, Hercules, CA) using the Bio-Rad substrate kit according to the manufacturer's instructions.

PTP assays. MBP and reduced carboxyamidomethylated and maleylated lysozyme (RCML) substrates were phosphorylated as previously described except that BIRK was used as the source of tyrosine kinase (Tonks et al., 1991). The assay buffer used was 25 mM imidazole, pH 7.2, 0.1% β-mercaptoethanol, and 5% glycerol containing 0.1% BSA. Assays were performed at 30°C for 6 minutes using 1 μM ^{32}P-tyrosine phosphate in a reaction volume of 30 μl. Reactions were terminated by adding 290 μl of a 10% activated, acid-washed Norit A charcoal (v/v) in 0.9N HCl, 0.1 M pyrophosphate, and 2 mM monosodium phosphate. The mixtures were centrifuged 3 minutes in a microfuge, and the supernatant counted. One unit of enzymatic activity is defined as 1 nmole of phosphate released per minute.

Immunodepletion of the rabbit polyclonal antiserum Ab205. SHP-1 was immobilized on AFFIGEL-102 beads (Bio-Rad) according to the manufacturer's protocol. The affinity resin was equilibrated in buffer E (10 mM imidazole, pH 7.2, 5% glycerol, 0.1% β-mercaptoethanol, and 1% BSA). The Ab205 antiserum (10 μm) was diluted tenfold in buffer E and diluted twofold with the SHP-1 affinity resin. The samples were then incubated end over end for 1 hour at room temperature. The depleted supernatant was saved and the beads recycled using 2 × 1-ml washes of 20 mM Tris/glycerin, pH 2.5, for 5 minutes, 2 × 1-ml washes of 1 M Tris-HCl, pH 7.5, for 1 minute, and 2 × 1-ml washes of buffer E. The saved supernatant was depleted twice

more as described above. An aliquot of each depletion round was diluted at a 1:2,000 final dilution and tested by dot-blot analysis. Three rounds of purification were sufficient to deplete this antiserum.

RESULTS

Deafferentation of the chicken auditory brainstem results in significant increases in SHP-1 immunostaining within NM by 36 hours following cochlea removal (Figs. 1C, 2). This increase is first observed 24 hours following deafferentation and continues to intensify through 3 days following the injury (Figs. 1B,C, 2). Figure 2 demonstrates that by 36 and 72 hours, a larger than tenfold increase in immunostaining occurs within the deafferented NM when compared to the unoperated, contralateral NM. The staining is nonneuronal and largely confined to NM itself. Clusters of small, stained glial cells located between neurons can be observed and some NM neurons are surrounded by darkly stained glial processes. This is most noticeable by 3 days following deafferentation (Fig. 1). Interestingly, there is a small increase in SHP-1+ glial cells within the brainstem in general at 3 days when compared to earlier time points.

SHP-1 immunostaining appears to reach a maximum around 3 days following cochlea removal. Figure 3 demonstrates that SHP-1 staining is decreasing in deafferented NM by day 6, with fewer SHP-1+ astrocytes present (Fig. 3A). By day 9, SHP-1 staining continues to decrease, although a few tissue sections show a sparse, punctate SHP-1 staining pattern (Fig. 3B). By day 13, SHP-1 immunoreactivity within NM has decreased to control levels (Fig. 3C).

Identification of SHP-1+ cells in NM

Control. Both the 205 and the 196 antisera label a very small number of glial cells throughout the chicken brainstem. The labeling is confined to the cytoplasm, confirming that SHP-1 has a cytoplasmic distribution in avian brain. The occasional immunopositive cell bodies and processes are uniformly distributed throughout the brainstem. Those glia that are immunopositive show a darkly labeled cytoplasm and staining in the proximal portion of their processes (Fig. 4A). Some glial cells surrounding blood vessels are also immunoreactive. The immunostained cells possess oval/round nuclei approximately 5 μm in diameter, which are characteristic of astrocytic nuclei. Antibodies to the astrocytic marker GFAP do not label all astrocytes in the chicken brainstem and experiments in vitro have shown that only those astrocytes containing very little GFAP are SHP-1+ (Sorbel and Lurie, personal communication). Therefore, identification of these cells as astrocytes must be based on their morphology. Figure 4 demonstrates that the nuclei of GFAP+ and SHP-1+ cells possess the same morphological characteristics, indicating that SHP-1+ cells in control brain are indeed astrocytes.

Within deafferented NM, the SHP-1+ glia also resemble astrocytes based on morphological criteria, and appear (at least initially) to represent a different population of cells than the GFAP+ astrocytes. The SHP-1+ cells contain the large, round nuclei characteristic of astrocytes (Fig. 4C). Alternate tissue sections taken from the same animal and counterstained with antibodies to GFAP demonstrate that the SHP-1+ nuclei look identical to those of GFAP+ astrocytes (Fig. 4D) and allow us to identify SHP-1+ cells as astrocytes within the deafferented brainstem.

Interestingly, SHP-1+ and GFAP+ astrocytes are located in different areas of NM at early times following deafferentation. When consecutive sections are immunostained with each antibody, this differential distribution is revealed. Six hours following deafferentation, GFAP+ astrocytes are found within the fiber tracts surrounding NM with a few stained processes penetrating the nucleus (Fig. 5B; Canady and Rubel, 1992; Rubel and MacDonald, 1992). Over time, GFAP immunoreactivity increases in the fiber tracts and begins to increase within NM (Fig. 5D). By 72 hours after deafferentation, there is a large increase in GFAP+ astrocytes both within and surrounding NM (Rubel and MacDonald, 1992; Lurie and Rubel, 1994; Fig. 5E). A very different pattern for SHP-1 is seen over time after deafferentation. Noticeably increased immunoreactivity for SHP-1 is not apparent until 18–24 hours following deafferentation and the increased staining is confined to within the boundaries of NM itself (Fig. 5A,B). By 72 hours, SHP-1+ astrocytes are largely found within the borders of NM whereas GFAP+ astrocytes are abundant both within NM and in the surrounding fiber tracts (Fig. 5C). It should be noted that at 3 days, some of the SHP-1+ astrocytes may also be GFAP+ based on their localization within NM. Additionally, our studies in vitro have found that astrocytes that express a lot of GFAP immunoreactivity do not show SHP-1 immunostaining whereas those astrocytes that express little GFAP are immunopositive for SHP-1 (Sorbel and Lurie, 1999).

Cell proliferation

Cochlea removal results in astrocyte proliferation as well as increased GFAP immunoreactivity within NM. However, there exists some variability among animals regarding the amount of glial proliferation that occurs in NM following cochlea removal; some animals exhibit a lot of glial proliferation whereas others do not. This may be related to the finding that many animals respond to deafferentation with a substantial amount of neuronal loss whereas others show much less cell death (Rubel et al., 1990). Importantly, those animals that exhibit a lot of astrocyte proliferation within NM following deafferentation show small increases in SHP-1 immunoreactivity within NM (Fig. 6A). In contrast, those animals that exhibit a small amount of astrocyte proliferation following deafferentation show a large increase in SHP-1 immunoreactivity within NM (Fig. 6B). These findings demonstrate that the amount of SHP-1 immunoreactivity expressed in NM following deafferentation is negatively correlated with the amount of proliferation expressed by each individual animal.

This leads to the idea that SHP-1 may play a role in the signaling cascade that regulates astrocyte proliferation. In order to examine whether SHP-1+ cells are those that do not enter the cell cycle following cochlea removal, animals received BrdU on days 2–3, 4–5, or 8–9 after deafferentation and were sacrificed 6 hours later. This procedure labels all cells that are in S-phase during the time BrdU is available. Astrocyte proliferation continues until

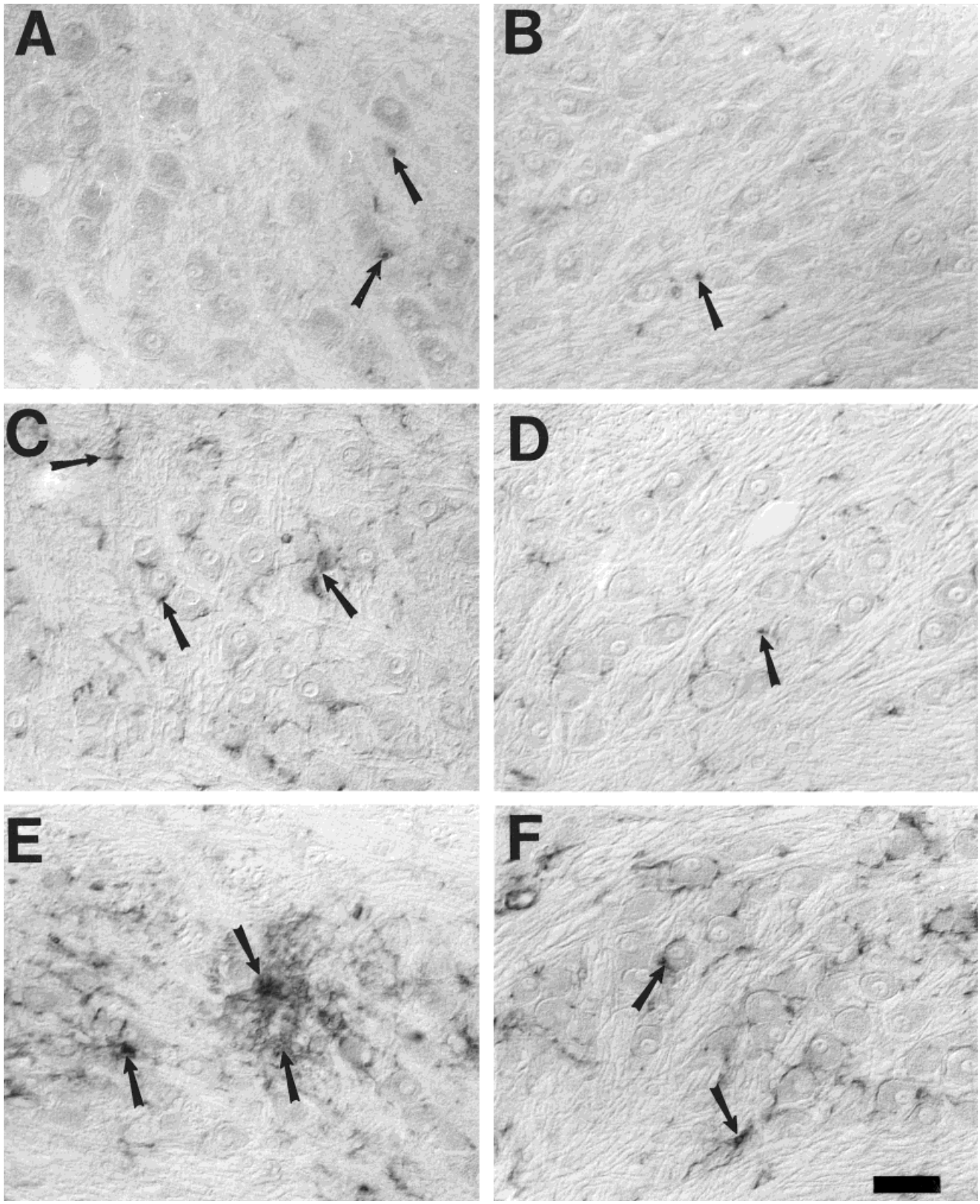

Fig. 1. SHP-1 immunoreactivity in NM following deafferentation. **A:** There are scattered immunopositive cells throughout the 6-hour deafferented NM (arrows). **B:** The contralateral unoperated side appears to have a similar number of immunopositive cells (arrow). **C:** At 24 hours, there is a small increase in the number of SHP-1+ positive astrocytes on the deafferented side (arrows) compared to the contralateral side (**D;** arrow). **E:** By 72 hours, there are many immunopositive astrocytes (arrows) on the deafferented side compared to the control side (**F;** arrows). Scale bar = 30 μm.

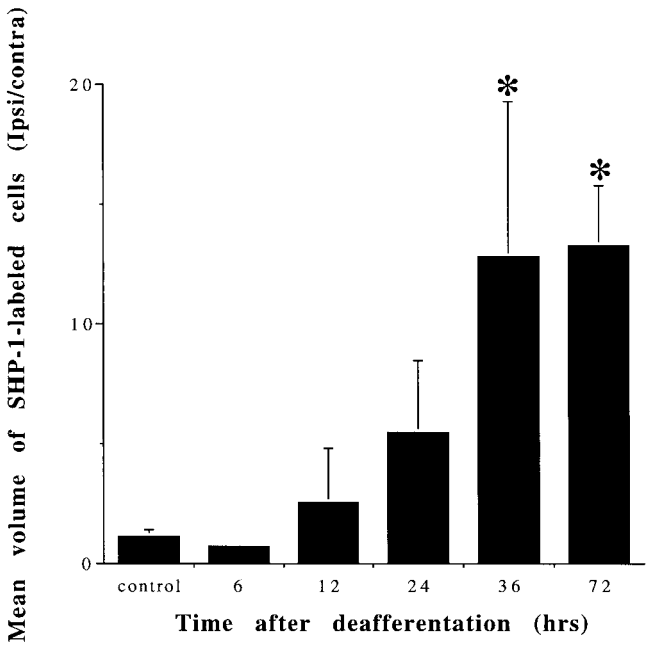

Fig. 2. The ratio of the mean volumes of SHP-1-immunolabeled astrocytes and their processes in the ipsilateral NM compared to the contralateral NM for control animals and animals sacrificed at 6, 12, 24, 36, and 72 hours after cochlea removal. There is a significant increase in the volume of SHP-1-immunolabeled astrocytes and their processes in the deafferented NM 36 hours after cochlea removal. Error bars indicate standard error of the mean. Asterisk, one-way ANOVA, $P \leq 0.05$.

at least day 9 following cochlea removal. Our results show that at all time points, the majority of the BrdU+ cells are SHP-1− and vice versa (Figs. 7A,B). However, occasional clusters of SHP-1+ cells with a BrdU+ nuclei at the edge of or within the cluster can be observed at all times following deafferentation (Fig. 7C). This pattern suggests to us that astrocyte proliferation is limited in areas that contain many SHP-1+ cells. SHP-1 may, therefore, play a role in negatively regulating the number of astrocytes that enter the cell cycle following deafferentation.

In order to quantify the negative relationship between SHP-1 and cell division, the number of BrdU+, SHP-1+, and BrdU+/SHP-1+ cells was counted in every section of all animals that received a pulse of BrdU as described in the Materials and Methods section. Animals that were allowed to recover from cochlea removal for 3, 6, and 9 days were pooled in order to obtain large numbers of labeled cells. Table 1 demonstrates that more than three times as many astrocytes are SHP-1+ as compared to BrdU-labeled cells. This indicates that smaller numbers of astrocytes proliferate in response to injury than increase SHP-1 immunoreactivity and do not enter the cell cycle. Interestingly, only 3% of all astrocytes appear to be double-labeled for both BrdU and SHP-1. It should be noted that the BrdU+ cells were often embedded in a cluster of SHP-1+ cells. It is impossible to determine whether such cells are actually double-labeled for both antibodies or whether one proliferating astrocyte is located within a group of SHP-1+ astrocytes. Therefore, it is likely that the actual number of actual double-labeled astrocytes is less than 3%.

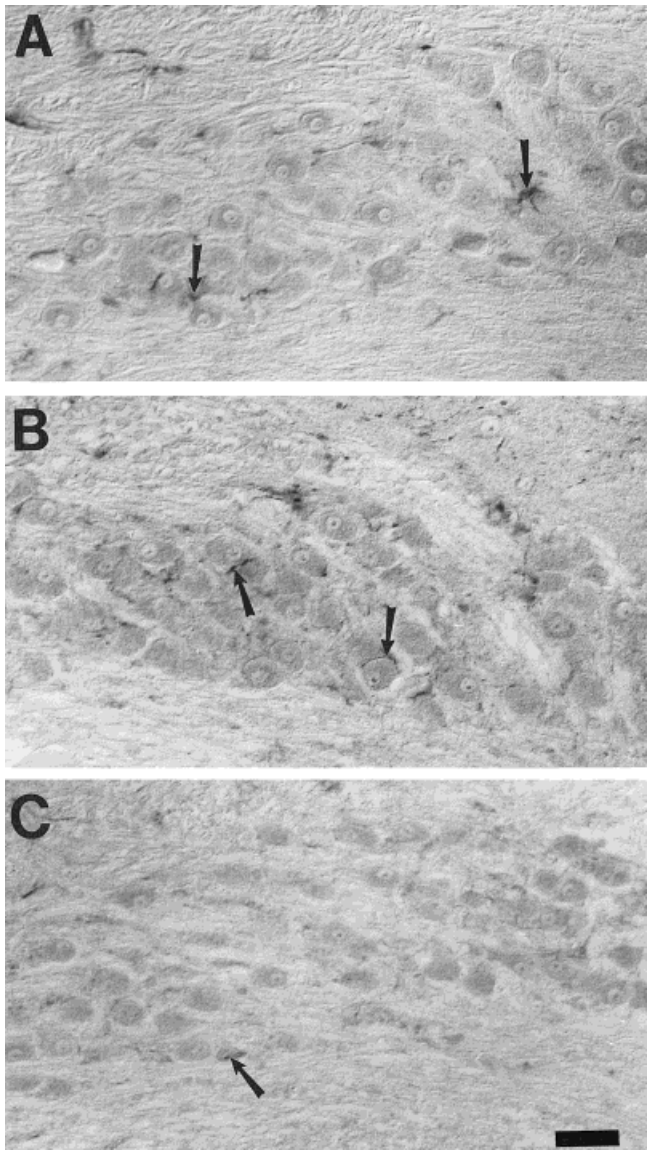

Fig. 3. SHP-1 immunoreactivity decreases in the deafferented NM over time. **A:** Deafferented NM 6 days following cochlea removal. A few SHP-1+ astrocytes can be seen (arrows), but there is much less SHP-1 immunoreactivity in NM as compared to 3 days after deafferentation. **B:** At 9 days following cochlea removal, a more punctate pattern of SHP-1 immunoreactivity can be observed in some tissue sections along with a few SHP-1+ processes (arrows). **C:** Very little SHP-1 immunoreactivity is found in the deafferented NM 13 days following cochlea removal (arrow) and levels of immunostaining are similar to the control NM. Scale bar = 30 μm.

Finally, we wanted to rule out the possibility that proliferating astrocytes differentiate into SHP-1+ astrocytes. Two animals were injected with BrdU on days 2 and 3 after cochlea removal and allowed to recover for 1 week following the last injection. The animals were then sacrificed and auditory brainstem sections processed for both BrdU and SHP-1 immunohistochemistry. Almost all of the astrocytes are positive for either BrdU or SHP-1 but not for both (Fig. 8). These results demonstrate that the ma-

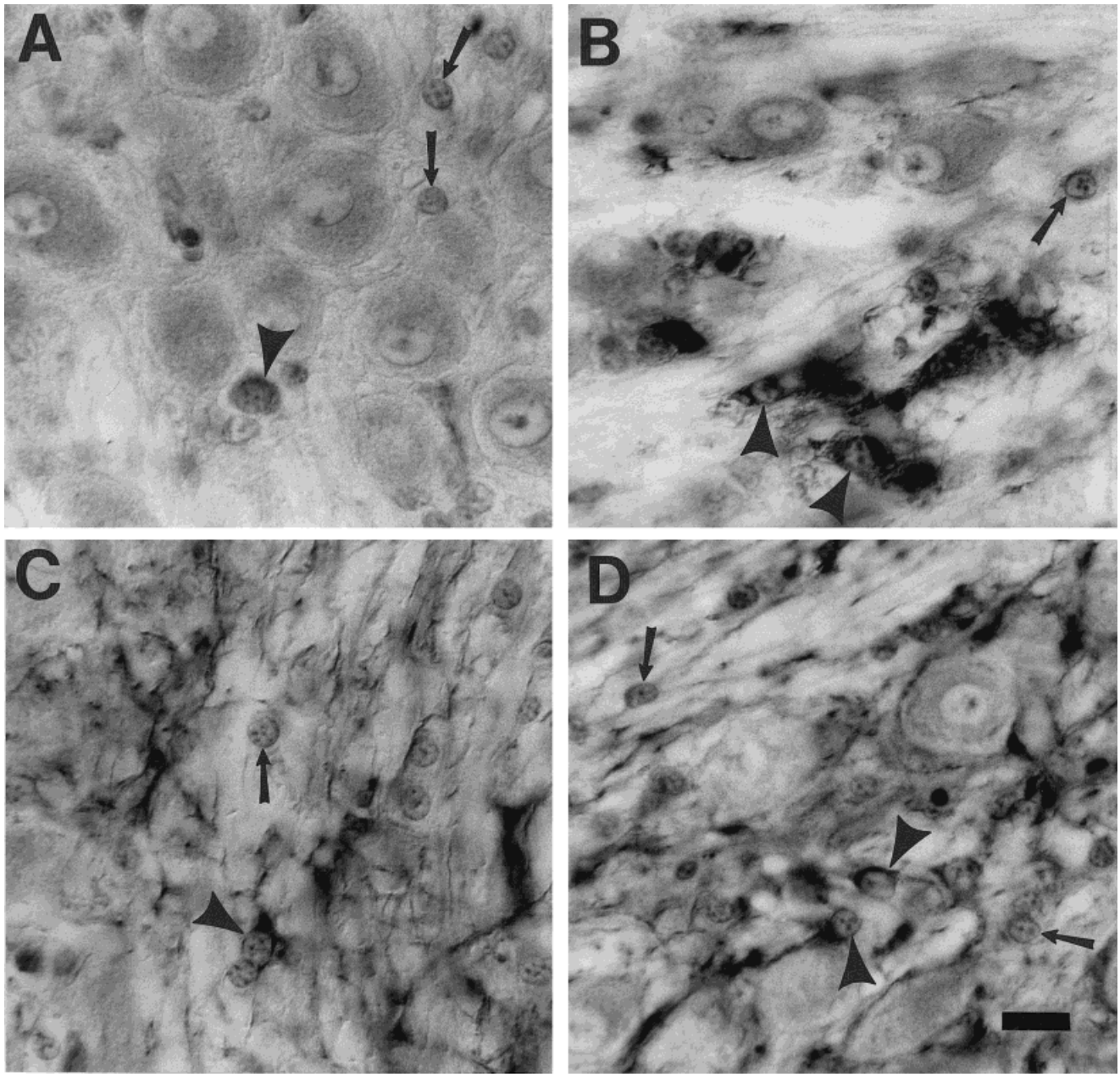

Fig. 4. SHP-1+ glia are astrocytes. Control NM counterstained with thionin and either SHP-1 or GFAP (A, C). **A:** Section immunolabeled with SHP-1 and counterstained with thionin. Note the large, pale nuclei characteristic of astrocytic nuclei (arrows). A single astrocyte is also very lightly immunolabeled for SHP-1 within the cytoplasm (arrowhead). **C:** Alternate section immunostained for GFAP and counterstained with thionin. Many astrocytes (large, pale nuclei) are positive for GFAP within the cytoplasm and glial processes (arrowhead). However, several astrocytes are not GFAP+ (arrow). Deafferented NM (3 days) counterstained with thionin and either SHP-1 or GFAP (B, D). **B:** Section immunolabeled with SHP-1 and counterstained with thionin. Note that the glial cells that show SHP-1 immunoreactivity within the cytoplasm possess the large, round, pale nuclei characteristic of astrocytes (arrowheads). There are several astrocytes located near the SHP-1+ cells that are not immunoreactive for SHP-1 (arrow). **D:** Alternate section immunolabeled with GFAP and counterstained with thionin. Many astrocytes are GFAP+ (arrowheads). However, even in the injured brainstem, there are many GFAP− astrocytes (arrows). Scale bar = 10 μm.

jority of proliferating astrocytes do not differentiate into SHP-1+ astrocytes.

Specificity of SHP-1 antibodies

Sequential anion exchange and sizing chromatography of chicken brain extracts with corresponding Western analysis show that the protein, SHP-1, is expressed in the chicken brain and is recognized by our antibodies. Because it is difficult to assign a particular PTPase activity to a specific phosphatase, we chose a purification scheme that had been previously used for the identification of SHP-1 in HL60 cells (Tonks et al., 1991). We found that

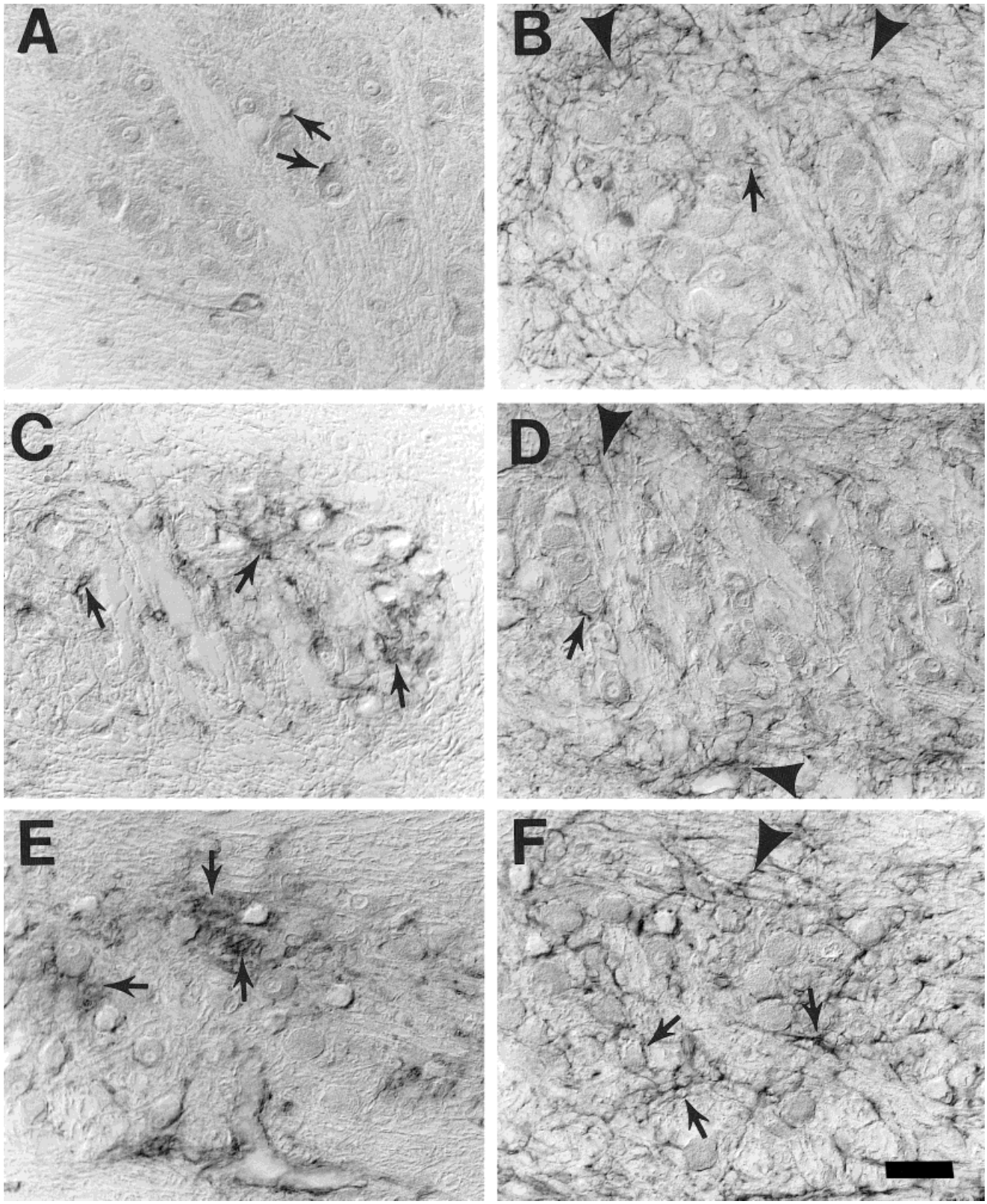

Figure 5

the SHP-1 activity from chicken brains elutes under similar conditions from the Q Sepharose Fast Flow column. Also, Western analysis performed on selected fractions demonstrates that fractions 12–18 are immunopositive for SHP-1 (Fig. 9). The immunopositive fractions correspond to the shoulder peak of phosphatase activity observed in the Q Fast Flow profile (Fig. 9).

In order to further confirm that the 68-kDa band corresponds with the PTPase activity, sizing chromatography was performed. Fractions 13–17 from the Q Fast Flow column were pooled and 1-ml aliquots were sized on a Superose 12 column. Fractions 22–29 were immunopositive for SHP-1. These fractions also correspond to the peak of phosphatase activity seen on the S12 profile (Fig. 10). The phosphatase activity elutes in fractions that correspond to the molecular weight of SHP-1 (approximately 66 kDa; Fig. 10).

Biochemical characterization

Finally, the effect of phosphatidylserine on the partially purified PTPase activity obtained from the Superose 12 fractionation shows that its activity behaves like that of SHP-1 (Zhao et al., 1994). Preincubation of the enzyme for 5 minutes in the presence of phosphatidylserine (167 ng/μm) resulted in an increase in the PTPase activity when MBP was used as the substrate (Fig. 11). With RCML as a substrate, inhibition of more than 50% is observed. Such behavior is characteristic for SHP-1 as phospholipids have been shown to induce a conformational change in SHP-1, which leads to increased activation when assayed with MBP (Zhao et al., 1993, 1994, 1995).

Histochemistry of SHP-1 antibody

To confirm the specificity of the SHP-1 antibody staining in the chicken, a depleted 205 antiserum was used to stain brain sections. Figure 12 demonstrates that when the 205 antiserum is passed over a SHP-1 affinity column in order to immobilize SHP-1-specific antibodies, there is a gradual loss of immunoreactivity with each pass over the column.

DISCUSSION

In control animals and at early times following deafferentation (<6 hours), a few uniformly distributed astrocytes throughout the chick brainstem are immunopositive for the tyrosine phosphatase, SHP-1. The number of SHP-1+ astrocytes increases over time following deafferentation. By 72 hours, many astrocytes and their processes within the damaged NM are darkly stained compared to the unoperated side. By 10–13 days following deafferentation, immunostaining for SHP-1 within NM has decreased to control levels, demonstrating that this increase is transient. Interestingly, there appears to be a mild increase in the number of SHP-1+ astrocytes in the entire chick brainstem at later times following deafferentation. This is not related to the anesthesia the animals receive (data not shown) but may indicate that unilateral loss of activity within NM influences the cellular environment of the whole chicken brainstem at the level of the auditory nuclei. Indeed, we and others have observed increases in both GFAP and BrdU labeling throughout the auditory brainstem at later times (2–3 days) following deafferentation (Lurie and Rubel, unpublished observations).

Two antibodies (205 and 196) raised against SHP-1 were found to label a subset of astrocytes in both control and damaged chicken brainstem. Both antisera recognize the enzyme in avian brain and depletion experiments confirm the specificity of the SHP-1 staining. The addition of phosphatidylserine on the partially purified PTPase obtained from the S12 fractionation shows that its activity behaves like that of SHP-1 (Zhao et al., 1993, 1994).

The finding that a subset of chick astrocytes becomes strongly immunopositive for SHP-1 following deafferentation is the first report of modulation of this enzyme in response to CNS damage. SHP-1 has been most thoroughly characterized in hematopoietic cells, where it is expressed at high levels and plays important physiological roles (Plutzky et al., 1992; Yi et al., 1993; David et al., 1995; Krautwald et al., 1996). However, SHP-1 has also been found in a variety of cells including human cervical carcinoma cells (You and Zhao, 1997), human epithelial carcinoma cells (Tomic et al., 1995), human embryonic kidney cells (Bouchard et al., 1994), rat liver cells (Ram and Waxman, 1997), rat pancreatic tumor cells (Cambillau et al., 1995), mouse astrocytes (Massa and Wu, 1996), and in P19 embryocarcinoma cells (Mizuno et al., 1997). It should be noted that both the signals that activate SHP-1 in vivo, as well as its substrates, are as yet unknown. In addition, the precise roles that SHP-1 plays in vivo have not been elucidated, although SHP-1 has been shown to be involved in growth factor-mediated signal transduction in nonlymphoid as well as hematopoietic cells (Yeung et al., 1992; Yi and Ihle, 1993; Bouchard et al., 1994).

Of particular relevance to the current study, IFN-γ has recently been shown to inhibit astrocyte proliferation both in vitro (DiProspero et al., 1997) and in vivo following a brain lesion (Pawlinski and Janeczko, 1997). Significantly, SHP-1 itself has been found to play a role in controlling the extent and duration of gene induction by IFN-γ through the JAK-STAT pathway in mouse astrocytes (Massa and Wu, 1996). This indicates that SHP-1 may act to limit astrocyte proliferation following brain injury in a number of different in vivo and in vitro models.

SHP-1 and cell division

Our data support the hypothesis that SHP-1 acts to negatively regulate astrocyte proliferation following

Fig. 5. Consecutive sections immunostained with GFAP and SHP-1. **A:** Six-hour deafferented NM immunolabeled for SHP-1. Note the immunostained cells are located primarily within NM (arrows). **B:** Six-hour deafferented NM immunolabeled for GFAP. There is an increase in GFAP immunoreactivity within the fiber tracts surrounding NM (arrowheads) and a small increase within NM itself (arrow). **C:** Twenty four-hour deafferented NM immunostained for SHP-1. There is an increase in the number of immunopositive astrocytes and their processes within NM (arrows). **D:** Twenty four-hour NM immunostained with GFAP. Note the increased GFAP immunoreactivity in the fiber tracts surrounding NM (arrowheads). At this time, there is also an increase in the number of GFAP+ fibers within NM (arrow). **E:** Seventy two-hour deafferented NM immunolabeled for SHP-1. There are many immunopositive astrocytes and processes within NM (arrows), however, the fiber tracts surrounding NM are relatively free of staining. **F:** Seventy two-hour deafferented NM immunostained with GFAP. There are many GFAP+ fibers both within NM (arrows) and in the surrounding fiber tracts (arrowhead). Scale bar = 30 μm.

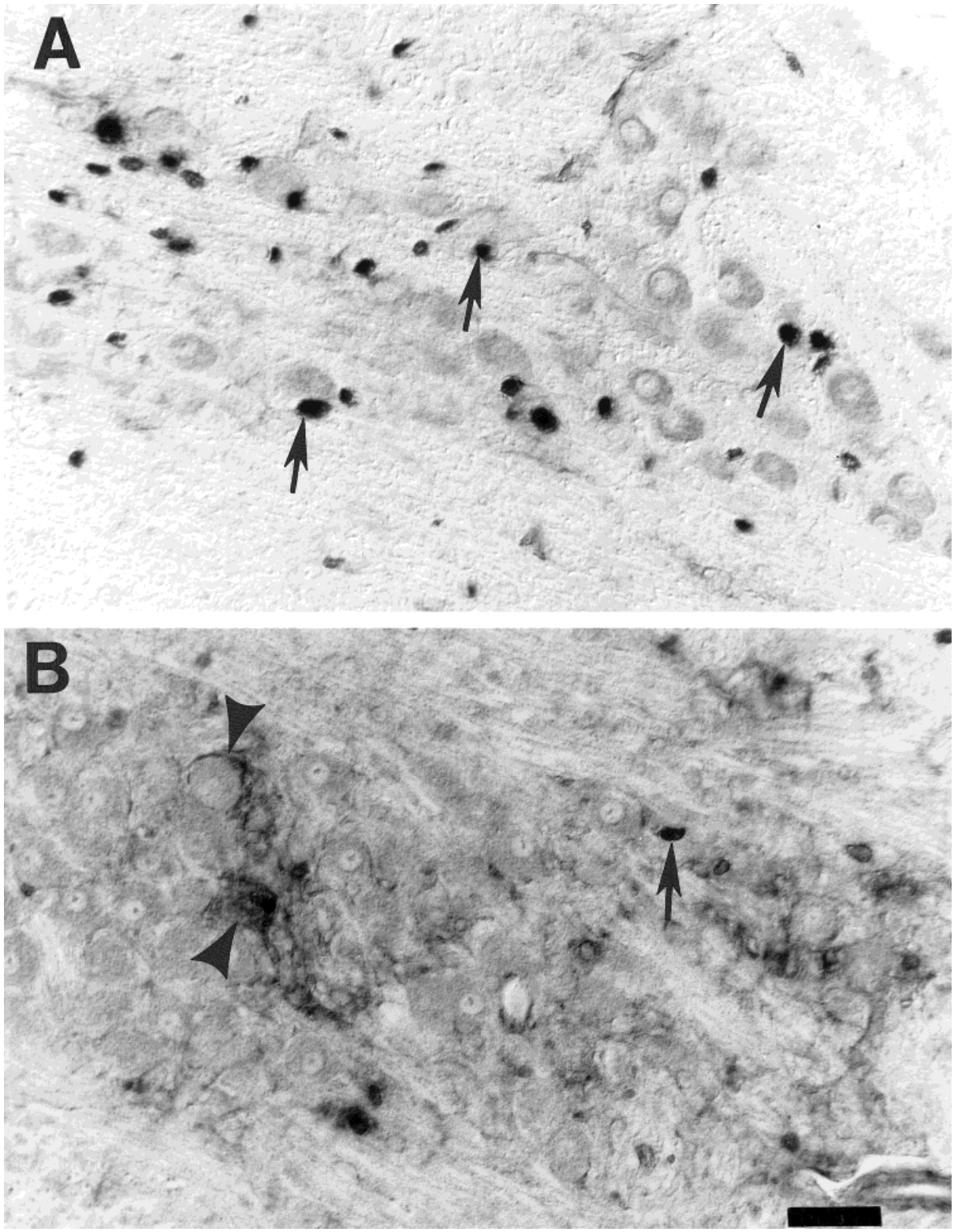

Fig. 6. Three days following deafferentation, animals that exhibit a large amount of astrocyte proliferation within NM have little SHP-1 immunoreactivity and vice versa. **A:** Deafferented NM labeled with BrdU on days 2–3. Note the large number of BrdU+ astrocytes (arrows) but almost no SHP-1 immunoreactivity. **B:** Deafferented NM from a different animal (pulsed with BrdU on days 2–3) demonstrating dense SHP-1 immunoreactivity (arrowheads) but much less astrocyte proliferation than the animal in (A) (arrow). Scale bar = 30 μm.

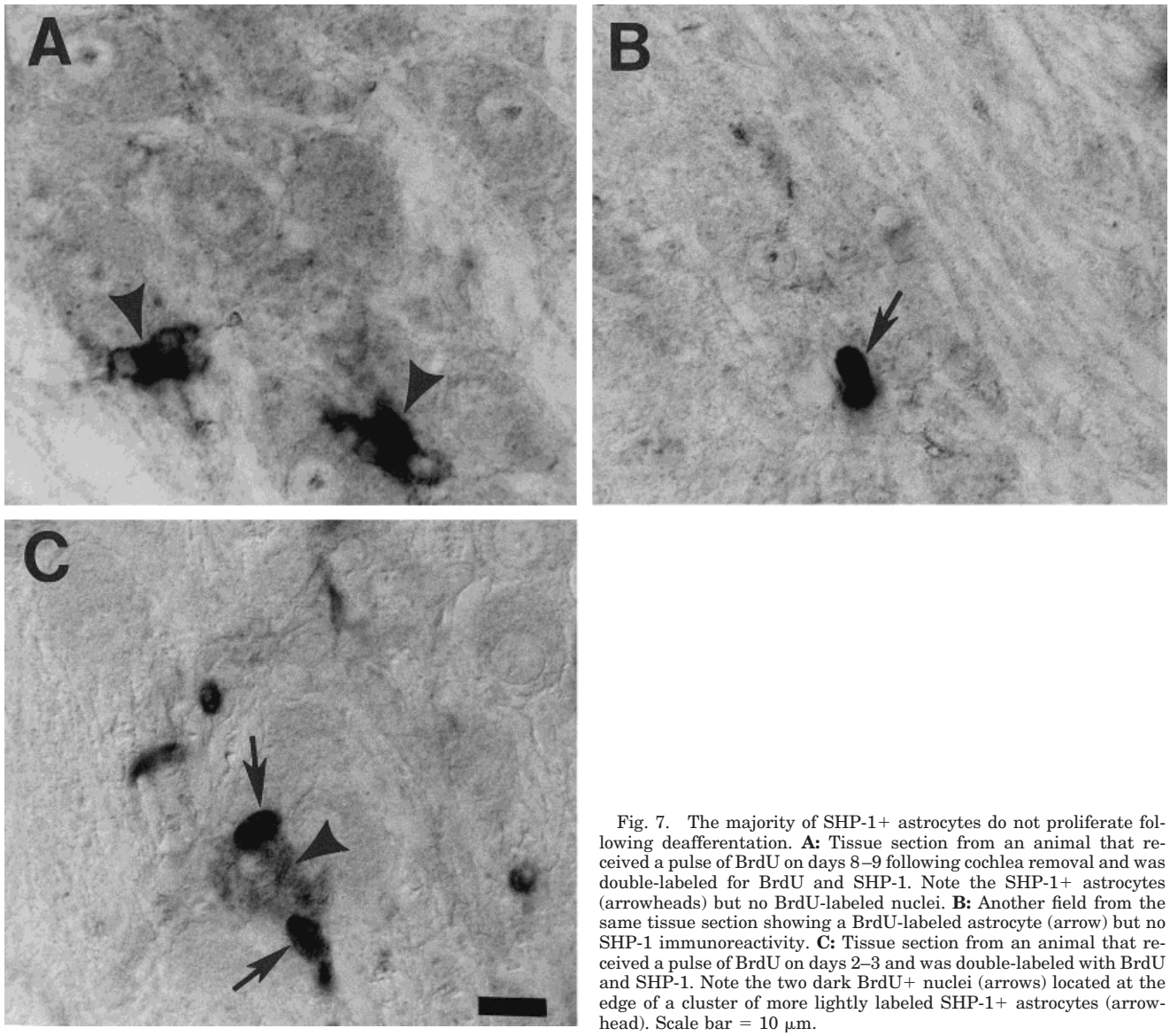

Fig. 7. The majority of SHP-1+ astrocytes do not proliferate following deafferentation. **A:** Tissue section from an animal that received a pulse of BrdU on days 8–9 following cochlea removal and was double-labeled for BrdU and SHP-1. Note the SHP-1+ astrocytes (arrowheads) but no BrdU-labeled nuclei. **B:** Another field from the same tissue section showing a BrdU-labeled astrocyte (arrow) but no SHP-1 immunoreactivity. **C:** Tissue section from an animal that received a pulse of BrdU on days 2–3 and was double-labeled with BrdU and SHP-1. Note the two dark BrdU+ nuclei (arrows) located at the edge of a cluster of more lightly labeled SHP-1+ astrocytes (arrowhead). Scale bar = 10 μm.

TABLE 1. BrdU+ vs. SHP-1+ Astrocytes Following Deafferentation in Animals Pulsed With BrdU[1]

	BrdU+	SHP-1+	BrdU+/SHP-1+
Number of astrocytes	787	2,630	111
Percent of total astrocytes counted	22%	75%	3%

[1]All animals that received a pulse of BrdU as previously described (n = 10) were pooled and the number of BrdU+, SHP-1+, and BrdU+/SHP-1+ astrocytes were counted. Note that more than three times as many astrocytes are SHP-1+ compared to BrdU-labeled astrocytes. In addition, only 3% of all astrocytes analyzed appear to be double labeled for both SHP-1 and BrdU.

deafferentation in the avian brainstem. However, we do observe some variability among animals in terms of both the number of proliferating astrocytes as well as the amount of SHP-1 immunostaining. This is likely to result from the variability in NM cell death that has been observed following cochlea removal. Twenty to 40% of NM neurons die following cochlea removal, with some animals exhibiting a substantial amount of cell loss whereas other animals show much less NM neuronal cell death (Rubel et al., 1990). Recent studies in adult birds have shown that neuronal cell death, rather than eighth nerve degeneration, is responsible for the increases in both the astrocyte proliferation and GFAP immunoreactivity that are observed in NM following deafferentation (Lurie and Durham, 1999). In the present study, those animals that respond to cochlea removal with substantial amounts of astrocyte proliferation show little SHP-1 immunoreactivity. Those animals with less astrocyte proliferation are heavily immunoreactive for SHP-1, indicating that SHP-1 may play a role in the signaling mechanisms that control the extent of glial proliferation following this injury.

In addition, a few BrdU+ astrocytes can be found among, or on the periphery of, many clusters of SHP-1+

Fig. 8. Proliferating astrocytes do not differentiate into SHP-1+ astrocytes. The NM from an animal that received a 6-hour pulse of BrdU 2 days following deafferentation, and then was allowed to survive for 1 week. The BrdU+ nuclei do not appear to be double-labeled with SHP-1 (large arrow). SHP-1+ astrocytes (small arrows) are not double-labeled with BrdU (note the cytoplasmic staining of SHP-1 with no nuclear labeling). Scale bar = 10 μm.

astrocytes at all times examined following deafferentation. This pattern demonstrates that astrocyte proliferation is limited in areas that contain many SHP-1+ glia and supports the idea that this enzyme negatively regulates astrocytic cell division. Studies in vitro also support this hypothesis. The addition of the PTP inhibitor sodium orthovanadate to mixed neural/glial cultures of the avian brainstem results in a dose-dependent increase in glial proliferation (Sorbel and Lurie, 1999), indicating that tyrosine phosphatase activity plays a role in preventing glial cells from entering the cell cycle.

Taken together, our findings are in agreement with studies in other systems where SHP-1 activity has been found to be inversely related to growth and proliferation of cells. As mentioned previously, IFN-γ inhibits astrocyte proliferation both in vitro and in vivo (DiProspero et al., 1997; Pawlinski and Janeczko, 1997). Somatostatin inhibits cellular proliferation and stimulates SHP-1 activity in Chinese hamster ovary cells (Lopez et al., 1997). The glucocorticoid dexamethasone inhibits proliferation of rat pancreatic tumor acinar cells and selectively increases SHP-1 expression and activity by severalfold (Cambillau et al., 1995). Phorbol esters inhibit the proliferation in human leukemia cells and stimulate expression and activity of SHP-1 (Uchida et al., 1993; Zhao et al., 1994).

In addition, the IL-3-induced growth stimulation of hematopoietic cells is suppressed by induction of SHP-1 expression (Yi et al., 1993). Loss of function mutations in the gene encoding SHP-1 result in the Motheaten and Viable Motheaten mouse phenotypes. In these animals, there is an increase in macrophage-like cells in the lymphoid tissue and bone marrow, as well as increased erythopoiesis (Bignon and Siminovitch, 1994). This suggests that under normal conditions when the enzyme is present, it serves to negatively regulate lymphocytic development.

However, a negative role for SHP-1 in growth and proliferation is not universal. Overexpression of SHP-1 in EGF-activated human embryonic kidney cells suggests a positive role for the phosphatase in mitogenic responses (Su et al., 1996). Proliferating P19 embryocarcinoma cells strongly express SHP-1, but treatment with retinoic acid results in the cessation of both SHP-1 expression and cell proliferation. In addition, constitutive expression of the phosphatase blocks the response to retinoic acid (Mizuno et al., 1997). Clearly, the role of SHP-1 in cell growth and

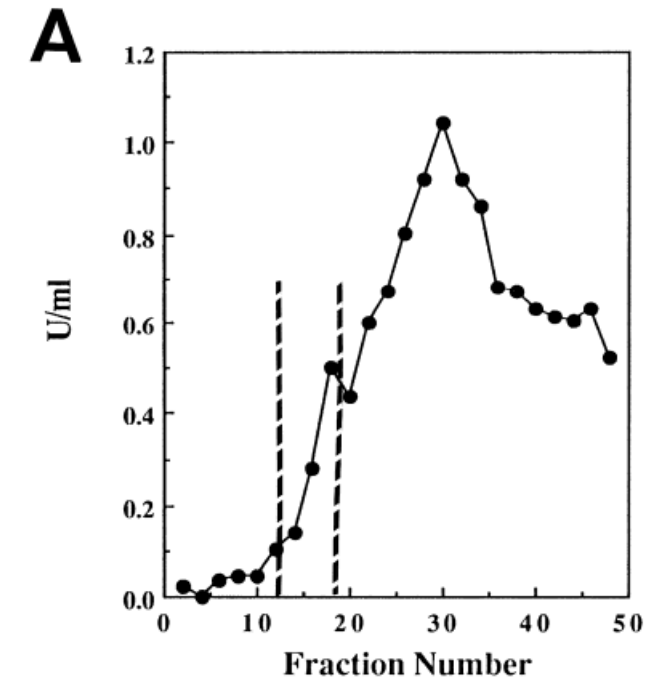

Fig. 9. Sequential anion exchange and sizing chromatography of chick brain extracts with corresponding Western analysis show that SHP-1 is expressed in the chick brain. **A:** PTP activity elution profile from a Fast Flow Q column. Tyrosine-phosphorylated MBP was used as the substrate. For details, see Materials and Methods. Fractions 12–18 (dotted lines) were selected for Western analysis. **B:** Western analysis of selected fractions from the Fast Flow Q profile using the anti-SHP-1 antiserum (205) as described in Materials and Methods.

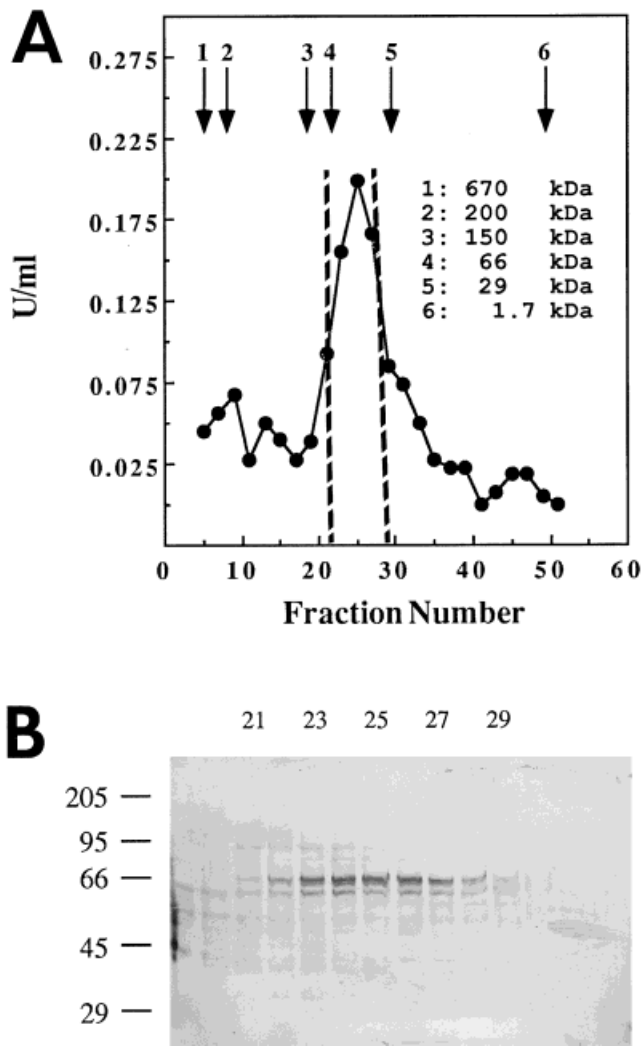

Fig. 10. The S12-Superose fractionation of the 205-immunoreactive pool obtained by Fast Flow Q chromatography. **A:** PTP activity elution profile from the S12-Superose column. Fractions 21–29 (dotted lines) were selected for Western analysis. Tyrosine-phosphorylated MBP was used as the substrate. **B:** Western analysis of the PTP activity peak observed on S12-Superose.

proliferation is dependent on cell type, signaling molecules, and other factors not yet identified.

Astrocyte response to deafferentation

Significant increases in proliferation, GFAP, and SHP-1 immunoreactivity all occur following deafferentation in the chicken auditory brainstem (Canady and Rubel, 1992; Rubel and MacDonald, 1992; Lurie and Rubel, 1994). However, different subsets of NM astrocytes exhibit at least two distinct responses to activity loss. One group of astrocytes responds to deafferentation by proliferating and then differentiating into GFAP+ astrocytes; the other shows large increases in SHP-1 immunoreactivity and these astrocytes do not proliferate. Our studies in vitro add support to this finding. In culture, auditory brainstem astrocytes that are heavily immunoreactive for GFAP do not label for SHP-1 and astrocytes that show very small amounts of GFAP staining are SHP-1+ (Sorbel and Lurie, 1999). However, it may be that astrocytes can switch expression of GFAP and SHP-1 and may have two inducible phenotypes depending on the signaling cascade. Further studies in vitro are needed to evaluate this possibility.

We do believe that neuronal cell death is an important mitotic signal for astrocyte proliferation, and that the large increases in both GFAP and SHP-1 immunoreactiv-

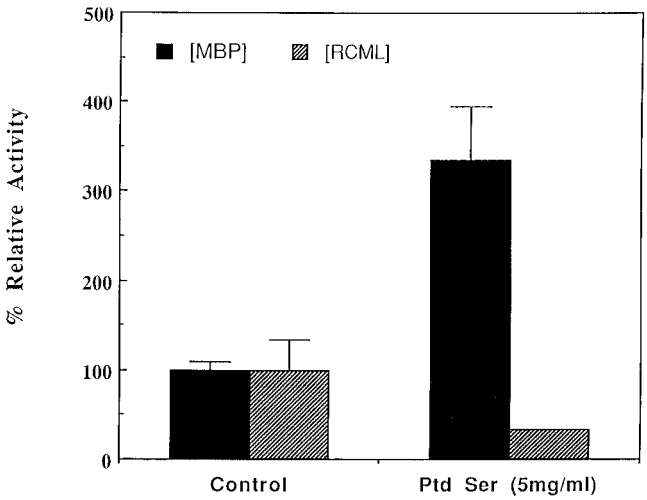

Fig. 11. The effect of phosphatidylserine on the partially purified PTP activity obtained from the S12-Superose fractionation shows that its activity behaves like that of SHP-1 (Zhao et al., 1993). Fraction 25 was used for the analysis and demonstrates that the relative PTP activity is increased at least three times over control when the enzyme is incubated with phosphatidylserine and MBP is used as the substrate. The SHP-1 activity does not increase with the addition of phosphatidylserine when RCML is used as the control substrate.

ity that we observe at later times following deafferentation are directly linked to this astrocytic division. However, it should be noted that both unilateral cochlea removal and unilateral eighth nerve activity blockade produce increased GFAP immunoreactivity *without* a concomitant increase in proliferation in some astrocytes as early as 1 hour following the manipulation. This increase is directly linked to the loss of neural activity and is reversible (Canady and Rubel, 1992; Rubel and MacDonald, 1992).

In summary, we hypothesize that SHP-1 is part of the intracellular cascade that is turned on to prevent some astrocytes from proliferating in the presence of an extrinsic signal to divide. When there is no such signal to divide, that is, in the uninjured brain, there is no need to upregulate SHP-1 and its expression remains low. Only when there is an intrinsic signal to divide does a regulatory mechanism become important, and SHP-1 is upregulated. Indeed, SHP-1 is also part of the glial response to injury in the mammalian CNS. We have observed increases in SHP-1 following both excitotoxic and metabolic lesion of the rat hippocampus (Willis et al., 1997), supporting the hypothesis that SHP-1 regulates glial proliferation following CNS injury in a number of different animal models. It will be of interest to determine whether neuronal debris can induce avian brainstem astrocytes to proliferate in vitro, as well as to determine whether inhibition of SHP-1 activity by tyrosine phosphatase inhibitors can increase the extent of astrocyte proliferation in response to this signal.

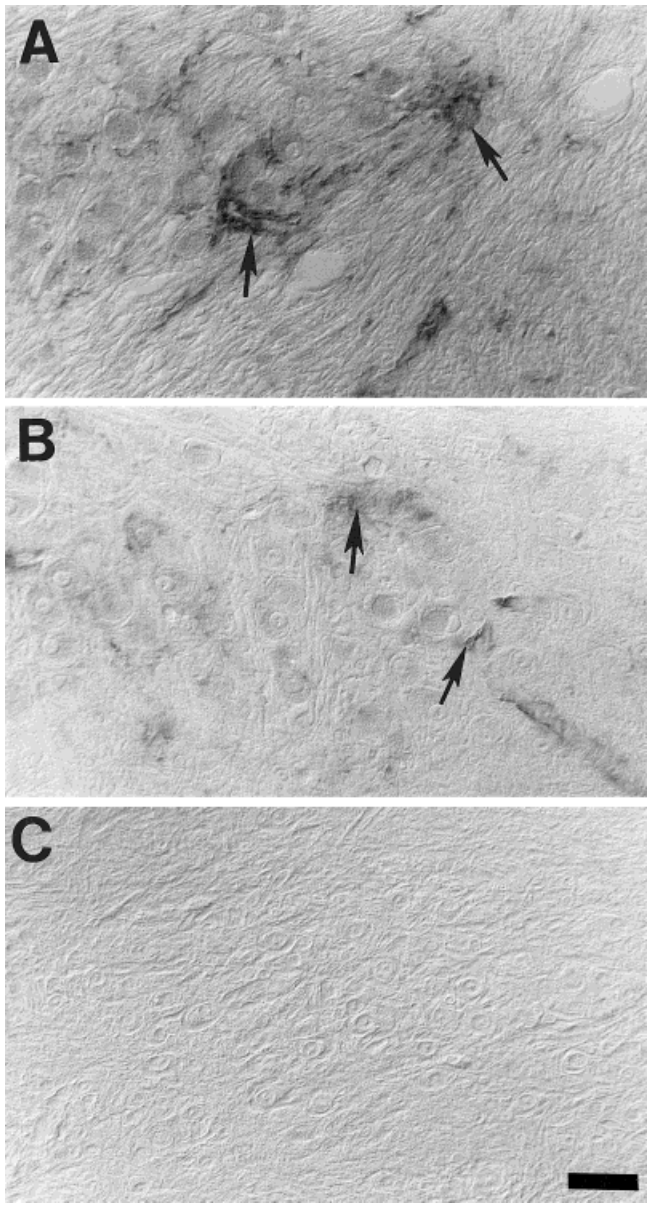

Fig. 12. When the 205 antiserum is passed over a SHP-1 affinity column in order to immobilize SHP-1-specific antibodies, there is a gradual loss of immunoreactivity with each passage over the column. **A:** Seventy two-hour deafferented NM immunostained with the 205 antiserum. Note the many immunostained glial cells and processes (arrows). **B:** Seventy two-hour deafferented NM immunostained with 205 antiserum that has been passed three times over the SHP-1 affinity column. Note the decreased intensity of immunostained glial cells (arrows). **C:** Seventy two-hour deafferented NM immunostained with 205 antisera that has been passed four times over the SHP-1 affinity column. Note the complete lack of immunostaining. The tissue samples used in A–C are consecutive sections through the NM. Scale bar = 30 μm.

ACKNOWLEDGMENTS

We thank Darla Kosena for her excellent technical assistance with immunocytochemistry, and Paul Shwartz and Janet Clardy for photographic assistance. We are also grateful to Dr. Shen for providing us with the 196 and 205 antibodies. This work was supported by NIH grants DC

00395 and DC 00520 (EWR), DK 07902 (EHF), and DC 02931 (DIL).

LITERATURE CITED

Bignon JS, Siminovitch KA. 1994. Identification of PTP1C mutation as the genetic defect in Motheaten and Viable Motheaten mice: A step toward defining the roles of protein tyrosine phosphatases in the regulation of hemopoiteic cell differentiation and function. Clin Immunol Immunopathol 73:168–179.

Born DE, Rubel EW. 1985. Afferent influences on brain stem auditory nuclei of the chicken: neuron number and size following cochlea removal. J Comp Neurol 231:435–445.

Bouchard P, Zhao Z, Banville D, Dumas F, Fischer EH, Shen S. 1994. Phosphorylation and identification of a major tyrosine phosphorylation site in protein tyrosine phosphatase 1C. J Biol Chem 269: 19585–19589.

Cambillau C, Rauly I, Sarfati P, Saint-Laurent N, Esteve J-P, Fanjul M, Svoboda M, Prats H, Hollande E, Vaysse N, Susini C. 1995. Regulation of the src homology 2 domain-containing protein tyrosine phosphatase PTP1C by glucocorticoids in rat pancreatic AR42J cells. Endocrinology 136:5476–5484.

Canady KS, Rubel EW. 1992. Rapid and reversible astrocytic reaction to afferent activity blockade in chick cochlear nucleus. J Neurosci 12: 1001–1009.

Condorelli DF, Ingrao F, Magri G, Bruno V, Nicoletti F, Avola R. 1989. Activation of excitatory amino acid receptors reduces thymidine incorporation and cell proliferation rate in primary cultures of astrocytes. Glia 2:67–69.

David M, Chen HE, Goelz S, Larner AC, Neel BG. 1995. Differential regulation of the alpha/beta interferon-stimulated Jak/Stat pathway by the SH2 domain-containing tyrosine phosphatase SHPTP1. Mol Cell Biol 15:7050–7058.

DiProspero NA, Meiners S, Geller HM. 1997. Inflammatory cytokines interact to modulate extracellular matrix and astrocytic support of neurite outgrowth. Exp Neurol 148:628–639.

Durham D, Rubel EW. 1985. Afferent influences on brain stem auditory nuclei of the chicken: changes in succinate dehydrogenase activity following cochlea removal. J Comp Neurol 231:446–456.

Graeber MB, Kreutzberg GW. 1986. Astrocytes increase in glial fibrillary acidic protein during retrograde changes of facial motor neurons. J Neurocytol 15:363–373.

Graeber MB, Kreutzberg GW. 1988. Delayed astrocyte reaction following facial nerve axotomy. J Neurocytol 17:209–220.

Harrison BC, Mobley PL. 1991. Phorbol myristate acetate and 8-bromocyclic AMP-induced phosphorylation of glial fibrillary acidic protein and vimentin in astrocytes: comparison of phosphorylation sites. J Neurochem 56:1723–1729.

Huff KR, Scheier W. 1990. Fibroblast growth factor inhibits epidermal growth factor-induced responses in rat astrocytes. Glia 3:193–204.

Ingraham CA, Maness PF. 1990. Tyrosine phosphorylated proteins decrease during differentiation of neuronal and glial cells. Dev Neurosci 12:273–285.

Kosena DK, Lurie DI. 1997. PTP1C and glial proliferation following deafferentation. Soc Neurosci Abs 23:67.

Krautwald S, Buschler D, Kummer V, Buder S, Baccarini M. 1996. Involvement of the protein tyrosine phosphatase SHP-1 in Ras-mediated activation of the mitogen-activated protein kinase pathway. Mol Cell Biol 16:5955–5963.

Langan TJ, Slater MS, Kelly K. 1994. Novel relationships of growth factors to the G1/S transition in cultured astrocytes from the rat forebrain. Glia 10:30–39.

Lau K-H, Baylink DJ. 1993. Phosphotyrosyl protein phosphatases: potential regulators of cell proliferation and differentiation. Crit Rev Oncogen 4:451–471.

Lopez F, Esteve J-P, Buscail L, Delesque N, Saint-Laurent N, Theveniau M, Nahmias C, Vaysse N, Susini C. 1997. The tyrosine phosphatase SHP-1 associates with the sst2 somatostatin receptor and is an essential component of sst2-mediated growth signaling. J Biol Chem 272: 24448–24454.

Lurie DI, Durham D. 1999. Unilateral cochlea removal results in increased GFAP within the avian auditory nucleus, nucleus magnocellularis, in adult egglayers but not broilers. Assoc Res Otolaryngol Abs 22:65.

Lurie DI, Rubel EW. 1994. Astrocyte proliferation in the chick auditory brainstem following cochlea removal. J Comp Neurol 346:276–288.

Lurie DI, Solca FF, Fischer EH, Rubel EW. 1993. Deafferentation results in increased glial immunoreactivity for a tyrosine phosphatase. Soc Neurosci Abs 19:446.

Malhotra SK, Shnitka TK, Elbrink J. 1990. Reactive astrocytes: a review. Cytobios 61:133–160.

Massa PT, Wu C. 1996. The role of protein tyrosine phosphatase SHP-1 in the regulation of IFN-γ signaling in neural cells. J Immunol 157:5139–5144.

Mizuno K, Katagiri T, Maruyama E, Kiminori H, Ogimoto M, Yakura H. 1997. SHP-1 is involved in neuronal differentiation of P19 embryonic carcinoma cells. FEBS Lett 417:6–12.

Neel BG. 1993. Structure and function of SH2-domain containing tyrosine phosphatases. Semin Cell Biol 4:419–432.

Pawlinski R, Janeczko K. 1997. Intracerebral injection of interferon-gamma inhibits the astrocyte proliferation following brain injury in the 6-day old rat. J Neurosci Res 50:1018–1022.

Plutzky J, Neel BG, Rosenberg RD. 1992. Isolation of a src homology 2-containing tyrosine phosphatase. Proc Natl Acad Sci USA 89:1123–1127.

Ram PA, Waxman DJ. 1997. Interactions of growth-hormone activated STATs with SH2-containing phosphotyrosine phosphatase SHP-1 and nuclear Jak2 tyrosine Kinase. J Biol Chem 272:17694–17702.

Reier PJ, Houle JD. 1988. The glial scar: its bearing on axonal elongation and transplantation approaches to CNS repair. In: Waxman SG, editor. Advances in neurology: functional recovery in neurological disease. New York: Raven Press. p 87–138.

Reier PJ, Stensaas LJ, Guth L. 1983. The astrocytic scar as an impediment to regeneration in the central nervous system. In: Kao CC, Bunge RP, Reier PJ, editors. Spinal cord regeneration. New York: Raven Press. p 164–195.

Rubel EW, MacDonald GH. 1992. Rapid growth of astrocytic processes in n. magnocellularis following cochlea removal. J Comp Neurol 318:415–425.

Rubel EW, Hyson RL, Durham D. 1990. Afferent regulation of neurons in the brain stem auditory system. J Neurobiol 21:169–196.

Shen S-H, Bastein L, Posner BI, Chetien P. 1991. A protein-tyrosine phosphatase with sequence similarity to the SH2 domain of the protein-tyrosine kinases. Nature 352:736–739.

Steward O, Torre ER, Phillips LL, Trimmer PA. 1990. The process of reinnervation in the dentate gyrus of adult rats: time course of increases in mRNA for glial fibrillary acidic protein. J Neurosci 10:2373–2384.

Su L, Zhao Z, Bouchard P, Banville D, Fischer EH, Krebs EG, Shen S-H. 1996. Positive effect of overexpressed protein tyrosine phosphatase PTP1C on mitogen-activated signaling in 293 cells. J Biol Chem 271: 10385–10390.

Tetzlaff W, Graeber MB, Bisby MA, Kreutzberg GW. 1988. Increased glial fibrillary acidic protein synthesis in astrocytes during retrograde reaction of the rat facial nucleus. Glia 1:90–95.

Tomic S, Greiser U, Lammers R, Kharitonenkov A, Imyanitov E, Ullrich A, Bohmer F-D. 1995. Association of SH2 domain protein tyrosine phosphatases with the epidermal growth factor receptor in human tumor cells. Phosphatidic acid activates receptor dephosphorylation by PTP1C. J Biol Chem 270:21277–21284.

Tonks NK, Diltz CD, Fischer EH. 1991. Purification of protein-tyrosine phosphatases from human placenta. Methods Enzymol 201:427–442.

Uchida T, Matozaki T, Matsuda K, Suzuki T, Matozaki S, Nakano O, Wada K, Konda Y, Sakamoto C, Kasuga M. 1993. Phorbol ester stimulates the activity of protein tyrosine phosphatase containing SH2 domains (PTP1C) in HL-60 leukemia cells by increasing gene expression. J Biol Chem 268:11845–11850.

Willis CL, Brunner KA, Bridges RJ, Lurie DI. 1997. Protein tyrosine phosphatase (PTP1C) expression in the rat hippocampus following injury. Soc Neurosci Abs 23:67.

Yeung Y-G, Berg KL, Pixley FJ, Angeletti RHM, Stanley ER. 1992. Protein tyrosine phosphatase-1C is rapidly phosphorylated in ty-

rosine in macrophages in response to colony-stimulating factor-1. J Biol Chem 267:23447–23450.

Yi T, Ihle JN. 1993. Association of hematopoietic cell phosphatase with c-kit after stimulation with c-kit ligand. Mol Cell Biol 13:3350–3358.

Yi T, Mui AL-F, Krystal G, Ihle JN. 1993. Hematopoietic cell phosphatase associates with the interleukin-3 (IL-3) receptor B chain and down-regulates IL-3-induced tyrosine phosphorylation and mitogenesis. Mol Cell Biol 13:7577–7586.

You M, Zhao Z. 1997. Positive effects of SH2 domain-containing tyrosine phosphatase SHP-1 on epidermal growth factor and interferon-γ-stimulated activation of STAT transcription factors in HeLa cells. J Biol Chem 272:23376–23381.

Zhao Z, Sheng S-H, Fischer EH. 1993. Stimulation by phospholipids of a protein-tyrosine-phosphatase containing two src homology 2 domains. Proc Natl Acad Sci USA 90:4251–4255.

Zhao Z, Shen S-H, Fischer EH. 1994. Phorbol ester-induced expression, phosphorylation, and translocation of protein-tyrosine-phosphatase 1C in HL-60 cells. Proc Natl Acad Sci USA 91:5007–5011.

Zhao Z, Shen S-H, Fischer EH. 1995. Structure, regulation, and function of SH2 domain-containing protein tyrosine phosphatases. Adv Prot Phosphatases 9:297–317.